Chiang Mai Dental Journal

Original Article

Effects of Mechanics for Uprighting Partially-Impacted Mandibular Second Molars using Miniscrew Anchorage: A Finite Element Analysis

Puttnaree Kittichaithanakoon[1], Virush Patanaporn[2], Chaiy Rungsiyakull[3]
[1]Graduate Student, Division of Orthodontics, Department of Orthodontics and Pediatric Dentistry, Faculty of Dentistry, Chiang Mai University, Thailand
[2]Department of Orthodontics and Pediatric Dentistry, Faculty of Dentistry, Chiang Mai University, Thailand
[3]Department of Mechanical Engineering, Faculty of Engineering, Chiang Mai University, Thailand

Received: June 1, 2021 • Revised: August 11, 2021 • Accepted: August 19, 2021

Corresponding Author: ***Clinical Professor Virush Patanaporn****, Department of Orthodontics and Pediatric Dentistry, Faculty of Dentistry, Chiang Mai University, Chiang Mai 50200, Thailand. (E-mail:* ***vr167420@hotmail.com****)*

Abstract

Objectives: The purposes of this study were: (1) to evaluate the optimal force magnitude that can be applied to the initial uprighting of partially-impacted mandibular second molar (tooth 37) without exceeding the hydrostatic pressure of the periodontal ligament (PDL) capillary vessels' blood pressure, which is 0.0047 megapascal (MPa) and distribution pattern of hydrostatic pressure on PDL 37; and (2) to describe initial tooth displacement of the impacted tooth 37, mandibular first molar (tooth 36) and mandibular second premolar (tooth 35) using the finite element method.

Materials and methods: A three-dimensional (3D) finite element model was developed from CBCT images. Various pushing forces, 35 to 150 g were applied to evaluate the optimal force magnitude. A force direction was laid from an interradicular miniscrew head, which was placed in the cortical bone between the root 35 and root 36, to a buccal minitube on the impacted tooth 37. The optimal force magnitude was used to simulate the initial tooth displacement of impacted tooth 37, tooth 36, and tooth 35.

Results: The optimal force magnitude, when a single-pushing-uprighting force applied, was 80 g. The compressive hydrostatic pressure on PDL 37 appeared on the disto-lingual region close to the cemento-enamel junction (CEJ); and the tension on PDL 37 appeared on the mesio-buccal side of the mesial root and on the mesio-buccal side of the distal root close to the furcation. The initial displacement pattern of the impacted tooth 37 was lingual crown tipping, distal crown tipping, distal root tipping, and disto-lingual rotation of the crown. It was found that the teeth 36 and 35 were also displaced, though force was not directly applied to them. Teeth 36 and 35 showed lingual crown tipping, extrusion, and distal crown tipping.

Conclusions: This finite element analysis was revealed that the force magnitude that can be applied to initial uprighting the mandibular second molar for this study was 80 g. The initial displacement pattern of the mandibular second molar, as descending order, was lingual crown tipping, distal crown tipping, distal root tipping and disto-lingual rotation of the crown. It was also revealed that the adjacent teeth were displaced, even though uprighting force was not directly applied to them.

Keywords: finite element method, impacted mandibular second molar, miniscrew anchorage, uprighting

Introduction

The prevalence of an impacted second mandibular molars varies from 0.06% to 2.3%, and is relatively rare.[1-3] Fu *et al.*[3] found that the initial angulation (defined as an angle between long axis of an impacted tooth and an adjacent first molar) of most impacted second mandibular molar ranged between 31° and 60°. This condition is irreversible and cannot be self-corrected.[4] To obtain proper occlusion, the permanent second molar should be positioned perpendicular to the occlusal plane, to resist occlusal force Uprighting of partially mesioangularly-impacted mandibular second molars is recommended, and should be accomplished as soon as possible.[5] If such impaction persists, it leads to adverse effects, including dental caries on the unerupted and neighboring teeth, external root resorption of adjacent teeth, cystic or neoplastic changes in the follicles of non-emerging impacted molars, overeruption of opposing teeth, occlusal interferences, traumatic occlusion, periodontal complications, such as difficulty in maintaining oral hygiene (especially on the mesial side), pseudopockets or vertical bone loss on the mesial surfaces of tipped mandibular molars.[5-10]

Orthodontically-assisted uprighting can be accomplished with or without surgical uncovering, depending on the position of the impacted molar.[6] The basic mechanics in the sagittal plane for orthodontic uprighting are distal crown tipping or mesial root movement.[11,12] In the conventional technique, the segmented or continuous archwire with pushed spring, cantilever spring,[8,12-15] T-loop spring,[11,16] NiTi-coil spring,[7] and super elastic NiTi wire[17] can be used. The conventional techniques often present a challenge for orthodontists because the unwanted movement of anterior anchorage units is difficult to control, not only in the sagittal, but also the vertical and horizontal, directions.[11,13] Nowadays, skeletal anchorage is widely used in orthodontic field, because it reduces side effects on dental anchorage units, simplifies orthodontic appliances and provides precise force systems, resulting in reduced treatment time.[5-7,18] The single pushing force (one dimensional force) for uprighting mechanics with skeletal anchorage was recommended in previous case studies[7,19] to release the mesial cusps of impacted teeth from the height of contour of adjacent teeth. However, the ultimate answer to the question of an optimal force system for the mechanics of uprighting impacted mandibular second molars has yet to be described.

Finite element (FE) analysis is a numerical method used for calculation of mechanical quantities to obtain approximate solutions. It is a noninvasive and reproducible technique. Hence, the FE method has been introduced as an effective tool for solving structural and biomechanical problems.[20]

The purposes of this study were: (1) to evaluate the optimal force magnitude that can be applied to the initial uprighting of partially mesioangularly-impacted mandibular second molars using single-pushing-force mechanics with miniscrew anchorage, without exceeding the hydrostatic pressure of the periodontal ligament (PDL) capillary vessel blood pressure, which is 0.0047 MPa;[21] and distribution pattern of hydrostatic pressure on PDL of the impacted tooth (2) to describe the initial tooth displacement using FE method, by which the model was reconstructed from cone beam computed tomography (CBCT) images.

Materials and Methods

A CBCT-based three-dimensional (3D) model for the FE analysis was obtained from a 12-year-old Thai boy who underwent orthodontic treatment at the Department of Orthodontics and Pediatric Dentistry, Faculty of Dentistry, Chiang Mai University and required pretreatment CBCT images. The CBCT images had met the following inclusion criteria: (1) a partially mesioangularly-impacted mandibular second molar; (2) enough bone distal to the target tooth for distal movement; (3) healthy periodontium and normal alveolar bone level; (4) No impeding third molar for uprighting mechanics. Exclusion criteria were: (1) root resorption; (2) abnormal crown or root morphology. The research purposes were explained to the study subject and his parents. Approval for this study was granted by the Human Experimentation Committee of the Faculty of Dentistry, Chiang Mai University, Thailand (No. 27/2018). The CBCT images of left mandibular area were produced using an ORTHOPHOS XG 3D/Ceph (Dentsply Sirona, New York, NY, USA) CBCT unit at 84 kV and 10 mA. Slice pitch was 0.16 mm, field of view was 5 cm x 5.5 cm and 0.16 mm voxel size. An initial angulation of tooth 37 was 55˚which is defined as an angle between long axis of the impacted tooth and the first molar (Figure 1).

The process of FE model construction is shown in Figure 2. The CBCT images were exported as Digital

Imaging and Communications in Medicine (DICOM) files and were converted to stereolithography (STL) files using the Mimics Research 17.0 software (Materialise, Leuven, Belgium). The 3D FE model consisted of a posterior part of left mandible, a left mandibular second premolar (tooth 35), a first molar (tooth 36), an impacted second molar (tooth 37), constructed PDL for each tooth, a buccal minitube, an adhesive, and a miniscrew head.

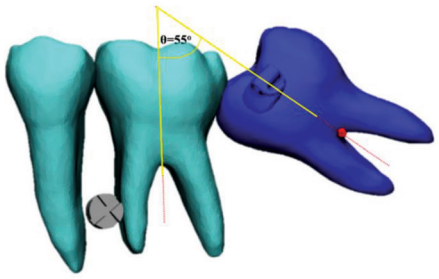

Figure 1: Initial angulation of impacted left permanent mandibular second molar is 55°.

The virtual PDL models were constructed around the root surface of each tooth with a 0.2-mm, uniform thickness,[22-25] using 3-Matic Research 9.0 software (Materialise, Leuven, Belgium). A buccal minitube (Victory Series™0.018" slot/066-4053 Stainless steel 3M®, St. Paul, Minnesota, USA), derived using a micro-CT scanner (SkyScan1173/11F05027, Bruker, Massachusetts, USA) as an STL file, was attached to tooth #37. An adhesive material, generated using 3-Matic software, lay between the buccal minitube and the tooth 37.

A miniscrew head was generated using SolidWorks software (Dassault Systemes, Waltham, MA, USA) and was placed in cortical bone between the root of tooth 36 and 35, 8.0 mm below the alveolar crest.[26]

The coordinate system of the whole 3D model was defined in order that the X-axis represented the antero-posterior (mesio-distal) direction, the Y-axis represented the vertical (gingivo-occlusal) direction, and the Z-axis represented the transverse (bucco-lingual) direction, with the positive direction to the buccal, occlusal, and distal direction, respectively (Figure 3). The final 3D model was imported to ABAQUS software (Dassault Systèmes, Waltham, MA, USA) and converted to a FE model.

The FE analysis was performed following these steps: (1) assignment of material properties; (2) definition of boundary condition and contact analysis; (3) definition of loading conditions; and (4) discretization (model meshing).

Firstly, the teeth, bone, attachment (buccal minitube), and adhesive were assigned as linearly homogenous materials as in previous FE studies.[27-32] The mechanical properties of the teeth, bone, attachment, and adhesive are shown in Table 1. The PDL was defined as a non-linearly elastic material using the Ogden constitutive model,[33] which provides strain energy calculation for the PDL. The third order of stain energy potential of the Ogden model[33] was applied is shown in Table 2.

Secondly, the boundary conditions were defined at peripheral nodes on the outer surface of the cortical bone. The contact condition between each structures of the FE model was assigned as tie-contact constraint. The tie-contact constraint was defined as the contact between each part of the model being perfectly bonded, but the surface on each part being separate.[34]

Table 1: Mechanical properties of tooth, cortical bone, stainless steel and adhesive[27-32].

Material	Young's modulus (MPa)	Poisson's ratio
Tooth	19600	0.30
Cortical bone	13700	0.26
Stainless steel	200000	0.3
Adhesive	8283	0.25

Table 2: Coefficients of third order Ogden constitutive model of PDL[33].

I	μ_i	α_i	D_i
1	-24.4237106	1.99994222	4.87164332
2	15.8966494	3.99994113	0.00000000
3	8.56953079	-2.00005453	0.00000000

Thirdly, for the assignment of the loading condition, this study mimicked the clinical situation from a previous case report study[7] that used the 0.016" stainless steel wire (as a core component) with open coil spring between miniscrew head and buccal minitube, to exert the single pushing force. The force direction of this study was a straight path from the midpoint of the interradicular miniscrew head to the midpoint of the buccal minitube slot on tooth 37 (Figure 3). Various force magnitudes of 35, 40, 50, 60, 70, 80, 90, 100, 120, 130, 140, and 150 g were applied to the mesial surface on the slot of buccal minitube on the tooth 37.

Fourthly, each part of the 3D model was divided into quadratic tetrahedron elements (type C3D10). The total

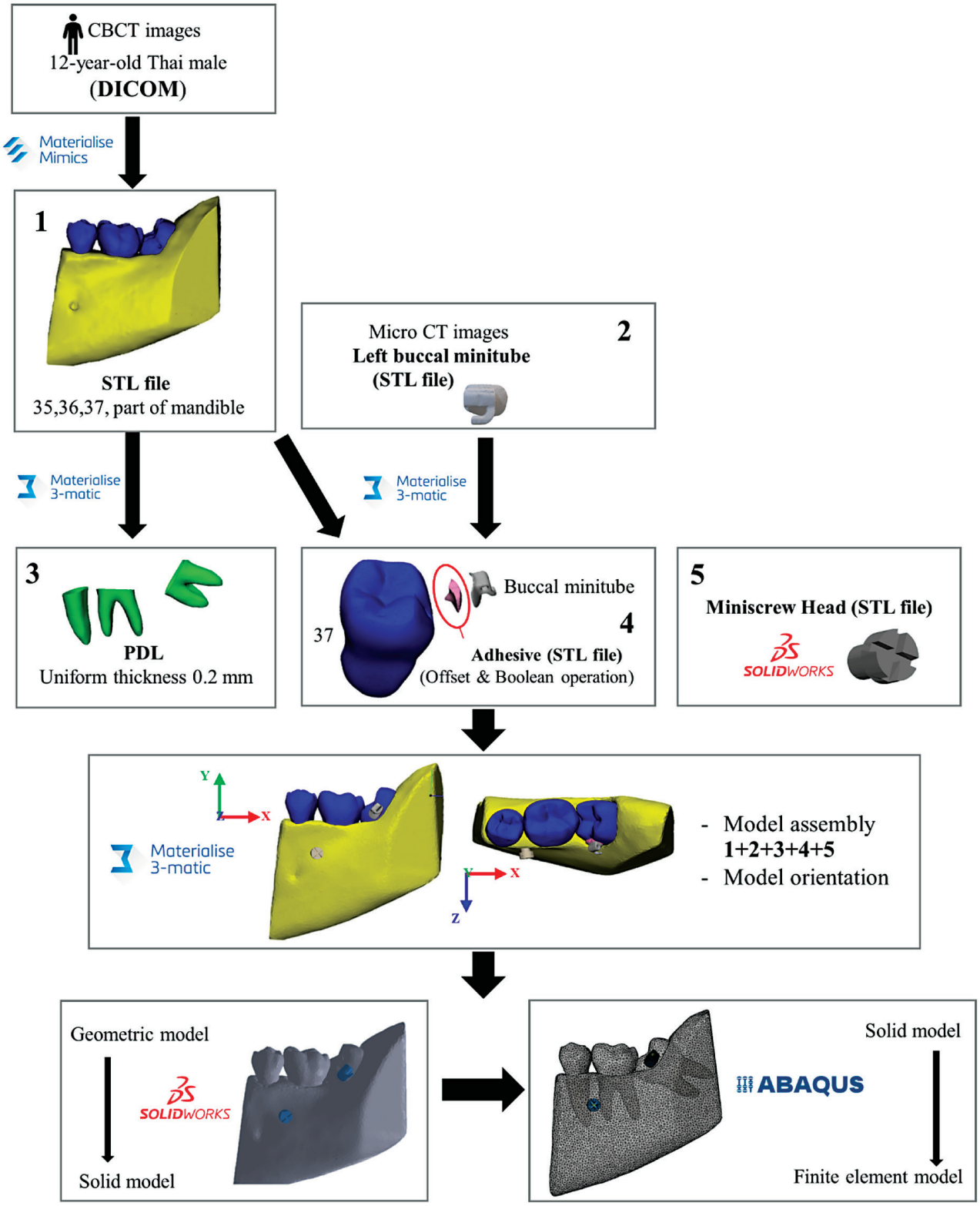

Figure 2: The process of FE model construction used in this study.

number of nodes and elements were 593,272 and 385,019, respectively.

Finite element analysis was performed: (1) the hydrostatic pressure (MPa) on the PDL 37 after the application of various force magnitude; and (2) the initial tooth displacement on impacted tooth 37, tooth 36, and tooth 35.

Results

1. Optimal force magnitudes and hydrostatic pressure pattern on the PDL of tooth 37

Force magnitudes of 35, 40, 50, 60, 70, 80, 90, 100, 120, 130 and 150 g were applied and the analysis revealed that when 80 g force was applied, a small red area of compressive pressure in which hydrostatic pressure equal to 0.0047 MPa (node 35609) appeared on the disto-lingual region close to the cemento-enamel junction (CEJ) of the PDL of the impacted tooth. Tension area (blue-colored area) appeared on the mesio-buccal side of the mesial root and on the mesio-buccal side the distal root close to the furcation (Figures 4, 5).

When the uprighting force magnitude was increased, the hydrostatic pressure pattern was similar to that when 80 g was used, but the compression and tension area of the PDL was widened (Figure 6).

The 80 g is the optimal force magnitude for single-pushing-uprighting mechanics of this study, and is equivalent to 0.0047 MPa of PDL capillary-vessel blood pressure.

2. Initial tooth displacement pattern of the impacted tooth 37, tooth 36, and tooth 35

The 80 g of force was selected to analyze the initial tooth displacement and the von Mises stress pattern in each tooth.

The numerical data for initial displacement in each axis of the crown and roots are shown in Table 3. Additionally, the superimposed images of tooth positions before and after uprighting force was applied are shown, with color-coded arrows, in Figure 7. The initial tooth position shows as light green shadow, and the final tooth position shows as blue opaque. The color-coded arrows represent the amount of tooth movement which was arranged from largest to smallest as red to blue arrows.

In summary, as descending order, tooth 37 showed lingual crown tipping, distal crown tipping, distal root tipping and disto-lingual rotation of the crown. Tooth 36 and 35 showed lingual crown tipping, extrusion, and distal crown tipping.

Discussion

1. Optimal force magnitude

This study demonstrated the optimal force magnitude that can be applied to the initial uprighting of partially mesioangularly-impacted mandibular second molars using single-pushing force mechanics with miniscrew anchorage, without exceeding the hydrostatic pressure of the PDL capillary vessel blood pressure, which is 0.0047 MPa,

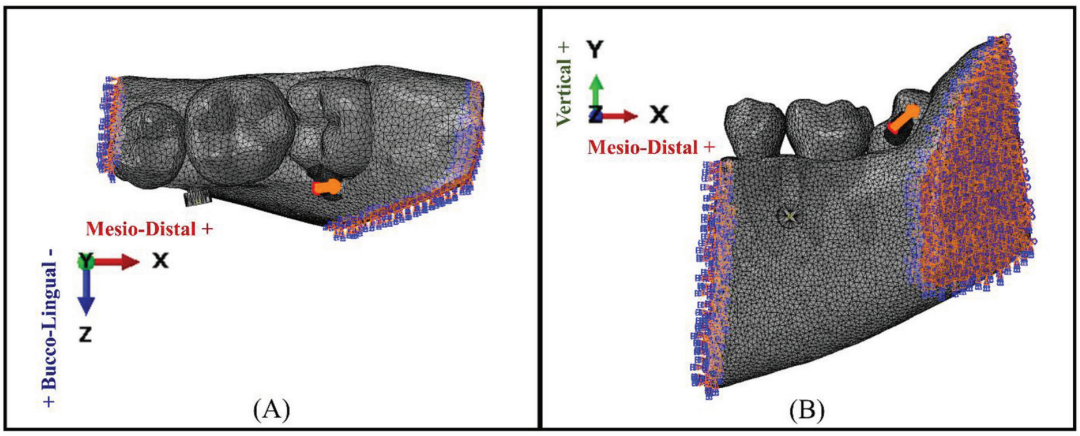

Figure 3: The force direction is shown as an orange arrow. The coordinated system of the three-dimensional model: X-axis representes the antero-posterior (mesio-distal) direction, the Y-axis representes the vertical (gingivo-occlusal) direction, and the Z-axis representes the transverse (bucco-lingual) direction. The boundary conditions are shown as orange-blue symbols (). (A) occlusal view, (B) buccal view.

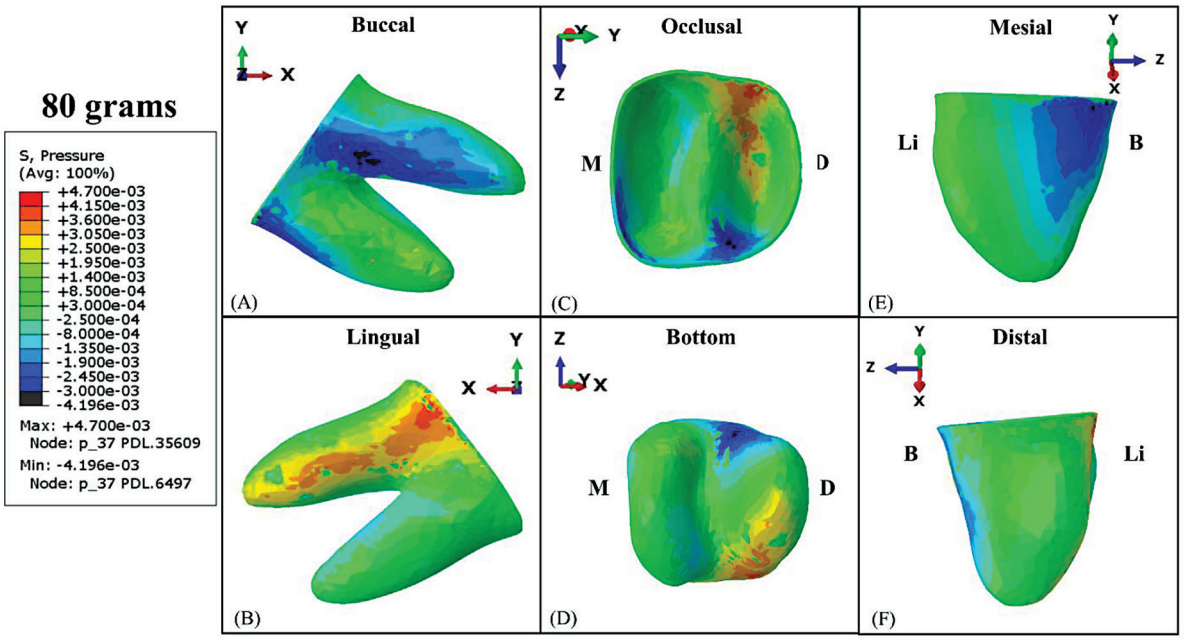

Figure 4: Color-coded map represents the hydrostatic pressure distribution along the periodontal ligament of impacted left permanent mandibularsecond molar when a single-pushing-uprighting force of 80 g is applied. M: Mesial, D: Distal, B: Buccal, Li: Lingual; (A) Buccal view, (B) Lingual view, (C) Occlusal view, (D) Bottom view, (E) Mesial view, (F) Distal view.

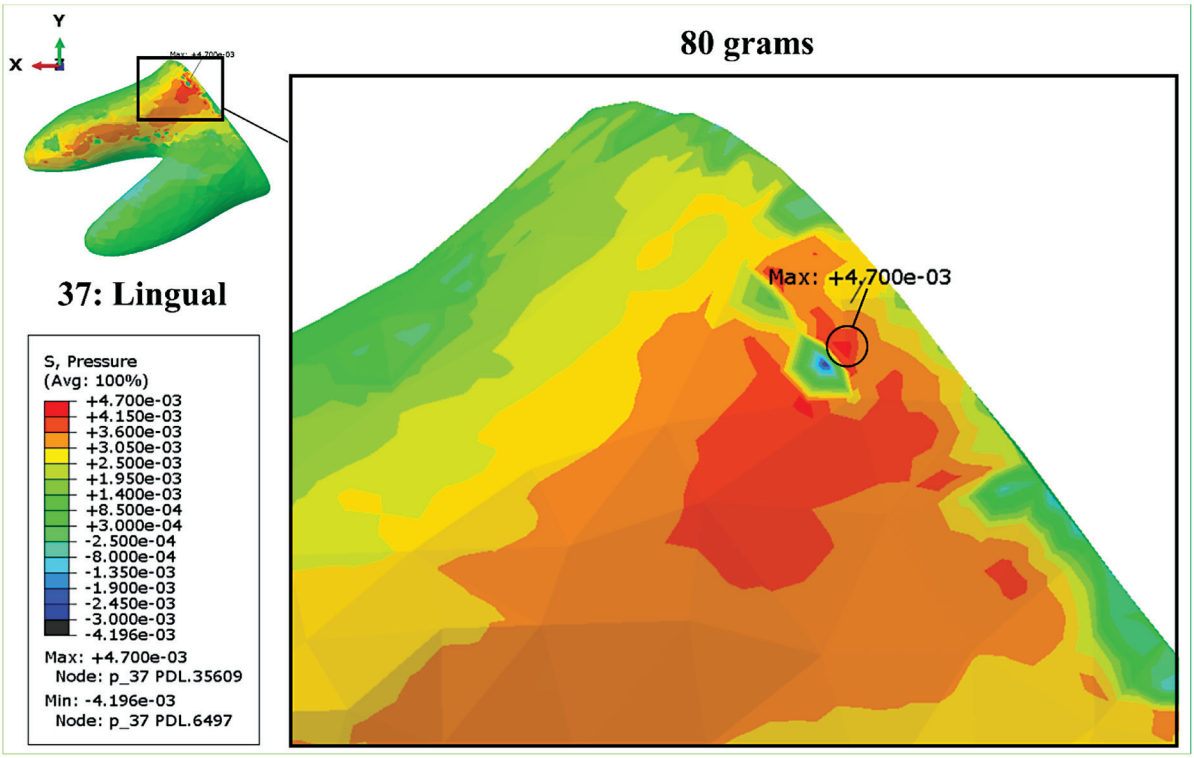

Figure 5: Magnified lingual view of periodontal ligament of impacted left permanent mandibular second molar after 80 g of pushing uprighting force was applied. The small red area shows the area which hydrostatic pressure equal to 0.0047 MPa (black circle outline).

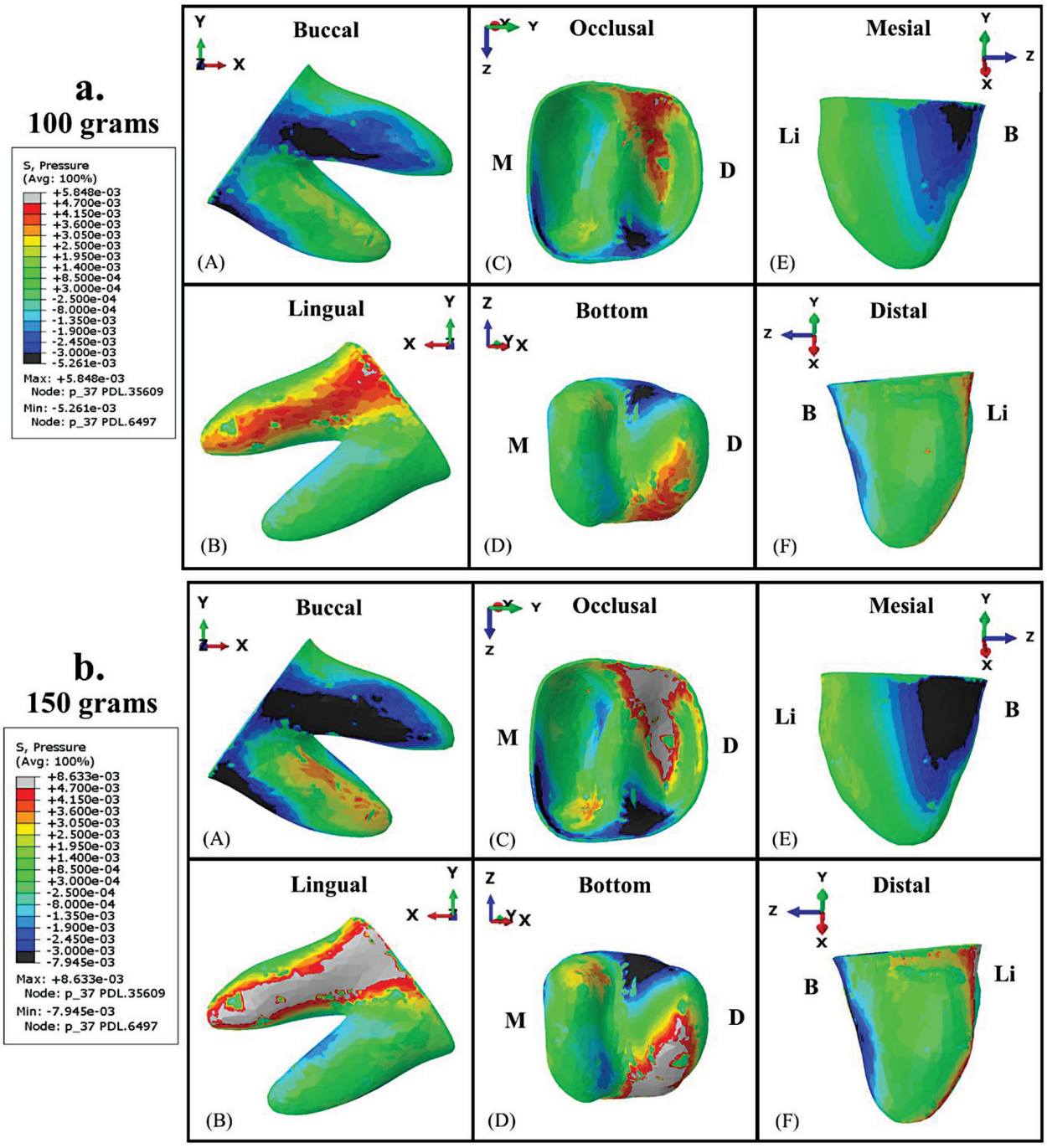

Figure 6: Color-coded map represent the hydrostatic pressure distribution along the periodontal ligamentof impacted left permanent mandibular second molar when an uprighting pushing force of 100g (6a) and 150g (6b) was applied. The gray color represents areas in which hydrostatic pressure exceeded 0.0047 MPa. M: Mesial, D: Distal, B: Buccal, Li: Lingual; (A) Buccal view, (B) Lingual view, (C) Occlusal view, (D) Bottom view, (E) Mesial view and (F) Distal view.

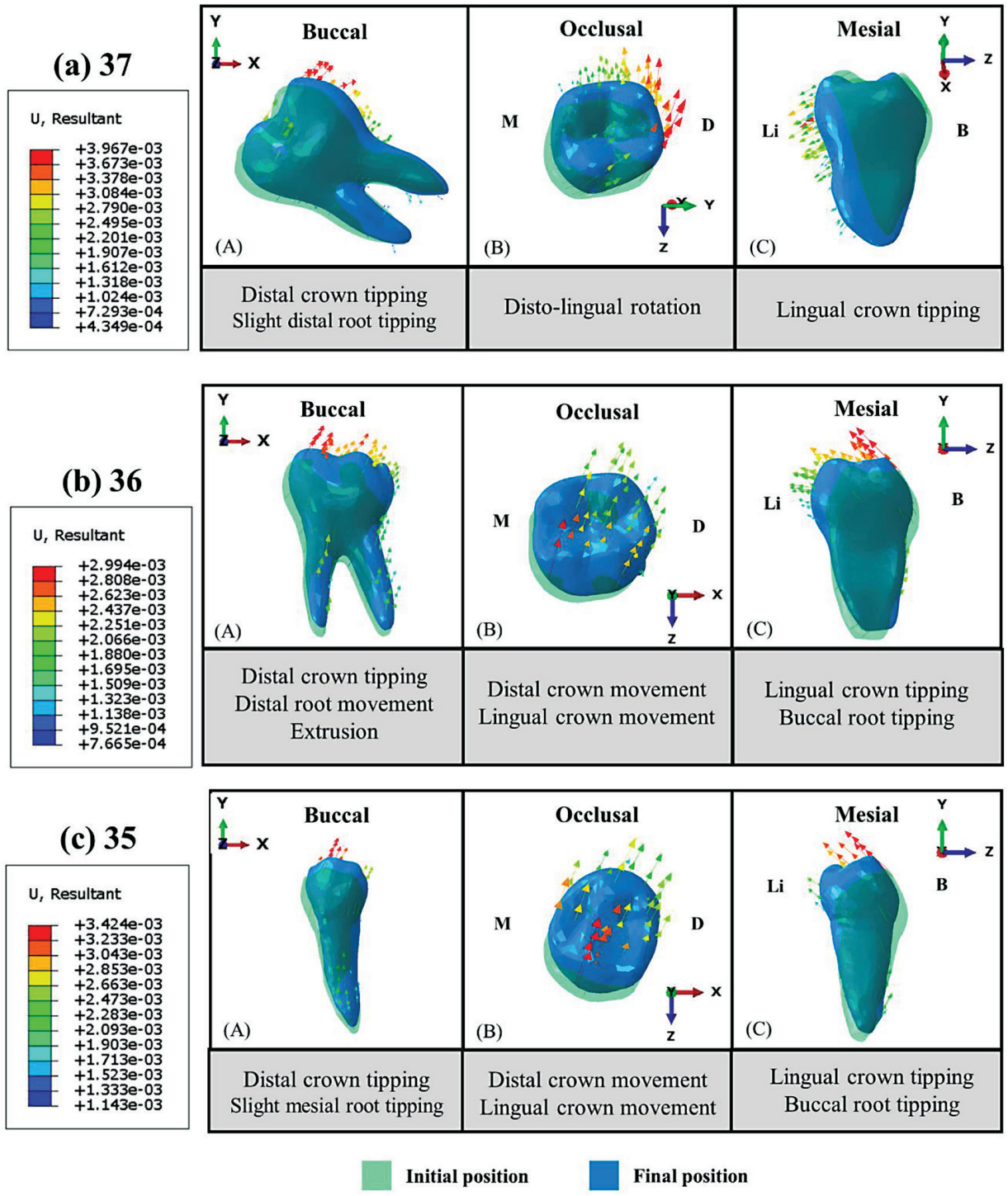

Figure 7: Initial displacement pattern of teeth (a) impacted left permanent mandibular second molar, (b) left permanent mandibular first molar and (c) left permanent mandibular second premolar. The light green shadow represents the initial position and the blue opaque represents the final position after single-pushing-uprighting force of 80 g was applied. Summaries of initial tooth displacement are described in the gray boxes below each diagram. M: Mesial, D: Distal, B: Buccal, Li: Lingual, (A) Buccal view, (B) Occlusal view and (C) Mesial view.

Table 3: Numerical data on initial displacement of teeth 37, 36, and 35 after a single pushing force of 80 g was applied: MBC, mesio-buccal cusp; DBC, disto-buccal cusp; MLC, mesio-lingual cusp; DLC, disto-lingual cusp; MRA, mesial root apex; DRA, distal root apex; RF, root furcation; BC, Buccal cusp; LC, Lingual cusp; MMR, mesial marginal ridge; DMR, distal marginal ridge; RA, root apex.

Tooth	Part	Location	Node No.	Displacement (in 10^{-3} mm)			Direction (descending order)
				ΔX	ΔY	ΔZ	
Impacted left permanent mandibular second molar (37)	Crown	MBC	387	0.93755	1.83931	-1.38248	Occluso-linguo-distal
		DBC	252	1.31068	1.68784	-3.06115	Linguo-occluso-distal
		MLC	304	0.77269	-0.27486	-1.51290	Linguo-disto-gingival
		DLC	172	1.16952	-0.26604	-3.24645	Linguo-disto-gingival
	Root	MRA	8659	0.24827	-0.06607	0.83334	Bucco-disto-gingival
		DRA	324	0.57597	-0.46236	-0.73065	Linguo-disto-gingival
		RF	30834	0.57706	0.20708	-0.47301	Disto-linguo-occlusal
Left permanent mandibular first molar (36)	Crown	MBC	15457	0.85401	1.86178	-2.16749	Linguo-occluso-distal
		DBC	130	0.86886	1.51882	-2.02001	Linguo-occluso-distal
		MLC	355	0.09983	0.79642	-2.18012	Linguo-occluso-distal
		DLC	14391	0.83696	1.71007	-1.96944	Linguo-occluso-distal
	Root	MRA	15203	0.16094	1.57543	1.45915	Occluso-bucco-distal
		DRA	409	0.15981	1.26835	1.62941	Bucco-occluso-distal
		RF	11240	0.51804	1.29928	0.02827	Occluso-distal-buccal
Left permanent mandibular second premolar (35)	Crown	BC	78	0.91979	2.31583	-2.34763	Linguo-occlusal-distal
		LC	11550	1.05040	1.33611	-2.26113	Linguo-occluso-distal
		MMR	12349	0.93990	1.67526	-2.10822	Linguo-occluso-distal
		DMR	8533	0.88769	1.64392	-1.97158	Linguo-occluso-distal
	Root	RA	4784	-0.39357	1.53208	1.37846	Occluso-bucco-mesial

was 80 g. One of the factors that receives high priority in orthodontic force systems is force magnitude.[35-37] Ren *et al.*[36] reported that the basic considerations of remodeling processes are not only the force magnitude but also the local stress and strain levels within the PDL. Thus, investigation of optimal stress/strain distribution within the PDL is pertinent. The PDL space is a continuous hydrostatic system and orthodontic force alters the hydrostatic pressure. Pressure is considered a special case of stress (force divided by area, F/A) which can be defined as a scalar (physical quantity that ignore direction), and is suitable for applying a load to gas or fluid inside a container. The hydrostatic pressure is the part of stress and can be determined by averaging the three axis of principle stress (compression and tension).[38] Yousefian *et al.*[39] suggested that the effect of positive and negative hydrostatic pressure is reciprocal to the compression site and tension site, respectively. The hydrostatic pressure is a suitable maker for PDL stress distribution, the data for which is provided by the FE analysis.

The ultimate answer to the question of an optimal force system for the mechanics of uprighting impacted second molars has not been concluded. Previous clinical case reports, that informed an amount of force level, using single force mechanics to upright second mandibular molars with miniscrews, have been reported. Giancotti *et al.*[19] used 50 g of single pulling force to upright a mandibular second molar with a retromolar miniscrew and a NiTi closed coil spring. Gracco *et al.*[40] used a distal jet appliance with a miniscrew in an edentulous area and 150 g activated a NiTi open coil spring. Two other clinical studies reported on molar tipping, which was not specific to molar uprighting, using force between 100 to 500 g.[41,42] Romeo and Burstone[43] recommended a value of moment of force for uprighting a single molar between 800 and 1,200 g.mm. Previous FE analysis study that determined the optimal force magnitude using single force (one way directed force) mechanics as this study, is not available.

To calculate the moment of force, the physical equation for a moment (M=Fxd; where M: moment, F: force,

d: distance perpendicular from the center of resistance to the line of force) can be practical. The approximate value of the moment of force (sagittal plane) produced by 80 g of single pushing force in this study was 568 g.mm with clockwise rotation (Figure 8).

Comparison between the result of optimal force magnitude from previous clinical case studies and this static FE analysis is difficult because the different of initial angulation and position of impacted molar, force direction and biological variation such as root morphology, periodontal status, and root surface area. These factors affect PDL stress distribution and optimal force magnitude.[36]

The result from this study can provide an estimate optimal force level using for initiating the single-pushing-uprighting mechanics of impacted tooth that resemble to this study.

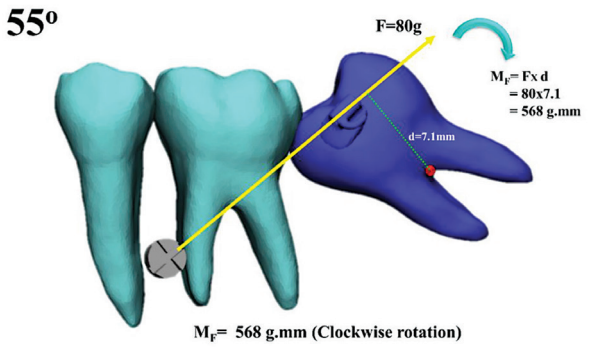

Figure 8: Moment of force (MF)(blue curve arrow) generated by 80 g of single-pushing-force (yellow arrow) and calculated from physical equation of moment (MF = F x d). The red dot represents the approximate position of the center of resistance. The moment of force in this study was 568 g.mm with clockwise rotation. MF: moment of force, F: force, d: perpendicular distance from the line of force to the center of resistance.

2. Initial tooth displacement of impacted tooth 37, tooth 36, and tooth 35

To describe the initial tooth displacement, the 80 g of single pushing force was applied. This study demonstrated that the initial displacement of the tooth 37, as descending order, was lingual crown tipping, distal crown tipping, distal root tipping and disto-lingual rotation of the crown. As the force direction was from the miniscrew to the buccal minitube on the tooth 37, and could not pass directly through its center of resistance (probably at the furcation or 1-2 mm apical to the furcation[44]), so a moment was produced and side effects in the vertical and bucco-lingual direction were unavoidable.

It is noteworthy that the initial displacement pattern of the impacted tooth 37 was coincident with the hydrostatic pressure pattern of its PDL. The disto-lingual area of the cervical third of the PDL represented the compression area (red, orange, and yellow patterns in the color-coded map) which concurred with disto-lingual rotation, and lingual and distal crown tipping of the initial tooth displacement pattern. Besides, the tension-stress areas in the PDL (green and blue patterns in the color-coded map) were shown in the mesio-buccal area of the mesial root at the cervical third level and the mesio-buccal area of the distal root at the cervical third level (Figure 9).

This study found that the teeth 36 and the 35 were displaced, though force was not directly applied to them. It is possible that the crown of the impacted tooth 37 lay under the height of contour of the first molar and when the target tooth was displaced, it affected the teeth 36 and 35. The tooth 35 was displaced to a greater degree than the tooth 36, even though the tooth 36 was closer to the target tooth than the tooth 35 was to the target tooth. The reason is because the low anchorage value of the second premolar compared to that of the first molar.[45,46]

3. Clinical application

There are two mechanics for orthodontically-assisted uprighting of impacted mandibular second molars: distal crown tipping and mesial root movement. Factors influencing the selection of these treatment mechanics are the treatment objective (space opening or closing), the initial position and angulation of the impacted teeth, and their root developmental stage.[6]

An impaction is defined as cessation of the eruption of a tooth, caused by a clinically or radiographically detectable physical barrier.[10,47] Mesial marginal ridge of impacted tooth usually locks under the height of contour of the first molar. Thus, treatment objective of the first step to correct an impacted condition should be moved the crown distally. Lee *et al.*[7] recommended that distal crown tipping mechanics, using single force (one way directed force) with direct miniscrew anchorage, utilized to unlock the impacted tooth from first molar. Additionally, in cases of mildly mesially-tipped molars, the moment of force produced by a single pushing force might be sufficient to generate distal crown tipping and be able to upright the

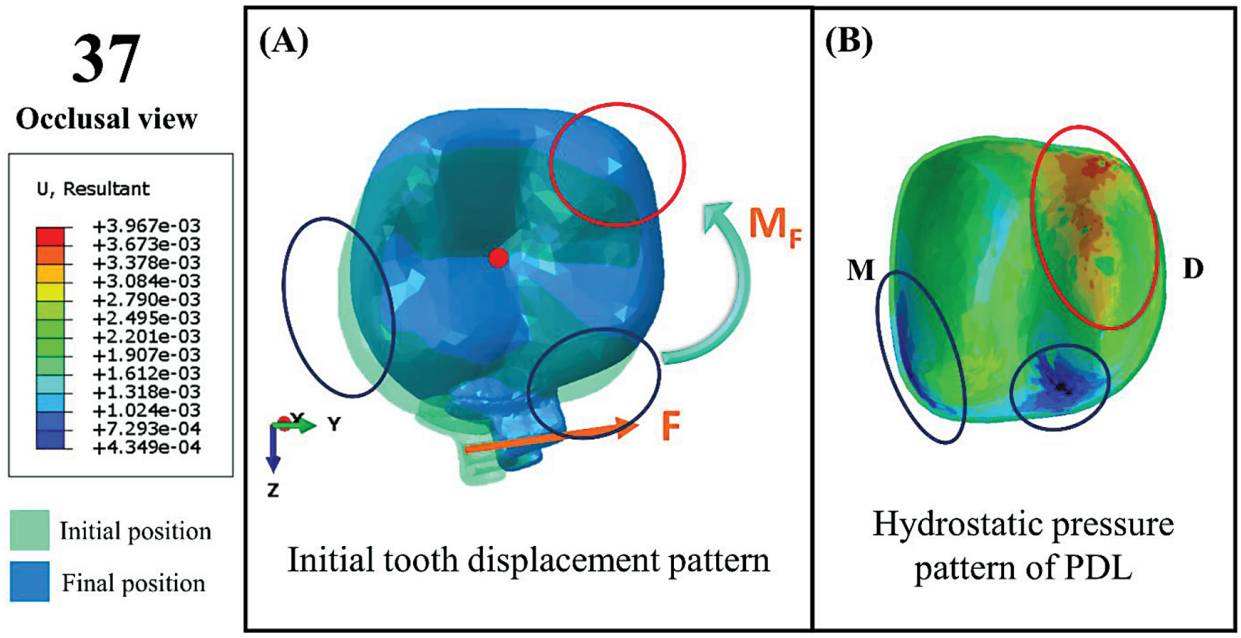

Figure 9: Occlusal view of Impacted left permanent mandibular second molar; (A) The initial displacement pattern (light green model shows the initial position, and the opaque blue model3-D shows the final position); (B) Color-coded map of hydrostatic pressure pattern of periodontal ligament of impacted left mandibular second molar. The initial displacement pattern is coincident with the hydrostatic pressure pattern of the periodontal ligament. Red-circle outlines show the compression area and blue-circle outlines show the tensile areas of the periodontal ligament. which concurred with the initial displacement pattern as disto-lingual crown rotation. F: Force, MF: Moment of force, M: Mesial, D: Distal.

impacted tooth, because of the greater distance from the line of force to the center of resistance, than in cases of severely mesially-tipped molars.[7,13]

This FE study revealed that the initial displacement of impacted tooth 37 as lingual crown tipping, which is an unwanted movement, were produced more than distal crown tipping. To reduce unwanted movement and to upright an impacted tooth into the ultimate position, adding a counteracting force as sequential application of different force system, is required. A full arch bonding of orthodontic brackets with rectangular main arch wire is suitable option to control impacted tooth movement in 3D direction especially when an initial angulation and position of impacted molar is three dimensionally malpositioned (lingually tipped, rotated, extruded).[5,7]

This FE study mimicked the clinical situation of a previous case study[7] that used an open coil spring with 0.016”stainless-steel wire as a core component to produce the single-pushing uprighting force. The final 3D model of this study was not constructed this wire because the force direction can be assigned as a straight path without the core component. However, in the clinical situation, the stainless-steel wire is placed into the slot of the buccal minitube, may affects the tooth movement pattern in latter phase which was not involved in this static FE study.

In summary, the use of single-pushing force with direct miniscrew anchorage for correction of mesially-impacted mandibular molar can be performed with carefully monitored the movement of impacted tooth, and modified the orthodontic force system when unwanted tooth movement is predicted or occurred.

4. Limitations of the study

The accuracy of a FE analysis depends on various factors. The difficulties of mimic biological structure are its irregular anatomy, non-elastic, anisotropic and heterogenous of biological materials behavior, boundary condition, shape, size and number of elements, and dynamic contact analysis.[34,48-51]

Limitation of this study was the assumption that the PDL and bone were homogeneous, isotropic and uniform in thickness. Additionally, the tooth-to-tooth contact condition which was assigned as a tie-contact constraint. In nature, tooth-to-tooth contact as sliding and friction phenomena during mastication, is highly non-linear.[34] These limitations can cause differences between simula-

tion studies and clinical applications.

This study was a static FE study which represented initial tooth movement. So, the results referred only to the first phase of tooth movement and did not refer to long-term tooth movement.[36]

To simulate the latter phase of tooth movement, and to clarify how initial position and angulation of an impacted tooth affects the optimal force magnitude and tooth displacement pattern of the single-pushing-uprighting mechanics, further dynamic FE studies are needed.

Conclusions

This FE study demonstrated that the optimal force magnitude that could be applied to initial uprighting the mesially-impacted permanent mandibular second molar using single-pushing force mechanics with direct miniscrew anchorage for this study, was 80 g. These results show that the hydrostatic pressure pattern on PDL of the impacted tooth was coincident with its initial tooth displacement pattern.

The initial displacement pattern of the permanent mandibular second molar, as descending order, was lingual crown tipping, distal crown tipping, distal root tipping and disto-lingual rotation of the crown. It is also revealed that the adjacent teeth were displaced, even though uprighting force was not directly applied to them. It may be concluded that the force exerted to the impacted tooth passed through its contact points to the adjacent teeth and produced 3D tooth movement in all three teeth. Hence, clinicians should consider the side effects of single-uprighting-force mechanics on not only the impacted second molar (target tooth) but also the adjacent teeth, for which counteract forces should be prepared to prevent unwanted movement.

Acknowledgements

The authors wish to thank the Department of Radiology, Faculty of Medicine, Siriraj Hospital, Mahidol University, for simulation software support and guidance throughout our study, and to the Department of Orthodontics and Pediatric Dentistry, Chiang Mai University, for the support in financial aid of this research. We would like to express our appreciation to Dr. M. Kevin O Carroll, Professor Emeritus of the University of Mississippi School of Dentistry, USA, and Faculty Consultant at Chiang Mai University, Faculty of Dentistry, for his assistance in the preparation of the manuscript.

References

1. Cassetta M, Altieri F, Di Mambro A, Galluccio G, Barbato E. Impaction of permanent mandibular second molar: A retrospective study. Med Oral Patol Oral Cir Bucal. 2013; 18(4):564.
2. Lau CK, Whang CZ, Bister D. Orthodontic uprighting of severely impacted mandibular second molars. Am J Orthod Dentofacial Orthop. 2013; 143(1):116-24.
3. Fu PS, Wang JC, Wu YM, Huang TK, Chen WC, Tseng YC, *et al*.Impacted mandibular second molars: A retrospective study of prevalence and treatment outcome. Angle Orthod. 2012;82(4):670-5.
4. Chintakanon K, Boonpinon P. Ectopic eruption of the first permanent molars: prevalence and etiologic factors. Angle Orthod. 1998;68(2):153-60.
5. Mah SJ, Won PJ, Nam JH, Kim EC, Kang YG. Uprighting mesially impacted mandibular molars with 2 miniscrews. Am J Orthod Dentofacial Orthop. 2015;148(5):849-61.
6. Sivolella S, Roberto M, Bressan P, Bressan E, Cernuschi S, Miotti F, *et al*. Uprighting of the impacted second mandibular molar with skeletal anchorage. In: Bourzgui F, ed: Orthodontics-Basic Aspects and Clinical Considerations. 1st ed. Rijeka: InTech; 2012:247-64.
7. Lee KJ, Park YC, Hwang WS, Seong EH. Uprighting mandibular second molars with direct miniscrew anchorage. J Clin Orthod. 2007;41(10):627-35.
8. Musilli M, Marsico M, Romanucci A, Grampone F. Molar uprighting with mini screws: comparison among different systems and relative biomechanical analysis. Prog Orthod. 2010;2(11):166-73.
9. Magkavali-Trikka P, Emmanouilidis G, Papadopoulos MA. Mandibular molar uprighting using orthodontic miniscrew implants: a systematic review. Prog Orthod. 2018; 19(1): 1-12.
10. Raghoebar G, Boering G, Vissink A, Stegenga B. Eruption disturbances of permanent molars: a review. J Oral Pathol Med. 1991;20(4):159-66.
11. Proffit WR, Sarver DM. Contemporary orthodontics appliances. In: Duncan L, ed: *Contemporary orthodontics*. 5th ed. Missouri: Elsevier Health Sciences; 2013:347-94.
12. Shellhart WC, Oesterle LJ. Uprighting molars without extrusion. J Am Dent Assoc. 1999;130(3):381-85.
13. Roberts III WW, Chacker FM, Burstone CJ. A segmental approach to mandibular molar uprighting. Am J Orthod. 1982;81(3):177-84.
14. Sawicka M, Racka Pilszak B, Rosnowska Mazurkiewicz A. Uprighting partially impacted permanent second molars. Angle Orthod. 2007;77(1):148-54.
15. Majourau A, Norton LA. Uprighting impacted second molars with segmented springs. Am J Orthod Dentofacial Orthop. 1995;107(3):235-38.

16. Tuncay OC, Biggerstaff RH, Cutcliffe JC, Berkowitz J. Molar uprighting with T-loop springs. J Am Dent Assoc. 1980;100(6):863-66.
17. Kim MH, Kim M, Chun YS. Molar uprighting by a nickel-titanium spring based on a setup model. Am J Orthod Dentofacial Orthop. 2014;146(1):119-23.
18. Lee KJ, Park YC. The biomechanics of miniscrews. In: Leah H, ed: *The biomechanical foundation of clinical orthodontics.* 1st ed. Hanover park: Quintessence Publishing; 2015: 433-50.
19. Giancotti A, Arcuri C, Barlattani A. Treatment of ectopic mandibular second molar with titanium miniscrews. Am J Orthod Dentofacial Orthop. 2004;126(1):113-17.
20. Rubin C, Krishnamurthy N, Capilouto E, Yi H. Stress analysis of the human tooth using a three-dimensional finite element model. J Dent Res. 1983;62(2):82-6.
21. Schwarz AM. Tissue changes incidental to orthodontic tooth movement. Int J Dent. 1932;18(4):331-52.
22. Kojima Y, Fukui H. Numeric simulations of en-masse space closure with sliding mechanics. Am J Orthod Dentofacial Orthop. 2010;138(6):702.e1- .e6.
23. Kojima Y, Fukui H. Numerical simulation of canine retraction by sliding mechanics. Am J Orthod Dentofacial Orthop. 2005;127(5):542-51.
24. Kojima Y, Mizuno T, Fukui H. A numerical simulation of tooth movement produced by molar uprighting spring. Am J Orthod Dentofacial Orthop. 2007;132(5):630-38.
25. Kojima Y, Takano M, Fukui H, Mizutani N, Hasegawa J. A simple method for calculating the initial tooth mobility and stress distribution in the periodontal ligament. Dent Mater J. 1999;18:210-16.
26. Bittencourt LP, Raymundo MV, Mucha JN. The optimal position for insertion of orthodontic miniscrews. Revista Odonto Ciência. 2011;26(2):133-38.
27. Borchers L, Reichart P. Three-dimensional stress distribution around a dental implant at different stages of interface development. J Dent Res. 1983;62(2):155-59.
28. Tanne K, Sakuda M, Burstone CJ. Three dimensional finite analyses for strss distribution in the periodontal tissue by orthodontic forces. Am J Dentofacial Orthop. 1987;92(6):499-505.
29. Cifter M, Sarac M. Maxillary posterior intrusion mechanics with mini-implant anchorage evaluated with the finite element method. Am J Orthod Dentofacial Orthop. 2011; 140(5):e233-41.
30. Toms SR, Eberhardt AW. A nonlinear finite element analysis of the periodontal ligament under orthodontic tooth loading. Am J Orthod Dentofacial Orthop. 2003;123(6):657-65.
31. Tanne K, Yoshida S, Kawata T, Sasaki A, Knox J, Jones ML. An evaluation of the biomechanical response of the tooth and periodontium to orthodontic forces in adolescent and adult subjects. Br J Orthod. 1998;25(2):109-15.
32. Williams K, Edmundson J. Orthodontic tooth movement analysed by the finite element method. Biomaterials. 1984;5(6):347-51.
33. Huang H, Tang W, Yan B, Wu B. Mechanical responses of Periodontal Ligament under a realistic orthodontic loading. Procedia Eng. 2012;31:828-33.
34. Murakami N, Wakabayashi N. Finite element contact analysis as a critical technique in dental biomechanics: a review. J Prosthodont Res. 2014;58(2):92-101.
35. Davidovitch Z. Tooth movement. Crit Rev Oral Biol Med. 1991; 2(4):411-50.
36. Ren Y, Maltha JC, Kuijpers-Jagtman AM. Optimum force magnitude for orthodontic tooth movement: a systematic literature review. Angle Orthod. 2003;73(1):86-92.
37. Melsen B. Tissue reaction to orthodontic tooth movement—a new paradigm. Eur J Orthod. 2001;23(6):671-81.
38. Viecilli RF. Stress, Strain, and the biological response. In: Leah H, ed: *The Biomechanical Foundation of clinical orthodontics.* 1st ed. Hanover park: Quintessence Publishing; 2015:209-226.
39. Yousefian J, Firouzian F, Shanfeld J, Ngan P, Lanese R, Davidovitch Z. A new experimental model for studying the response of periodontal ligament cells to hydrostatic pressure. Am J Orthod Dentofacial Orthop. 1995; 108(4):402-09.
40. Gracco A, Lombardo L, Cozzani M, Siciliani G. Uprighting mesially inclined mandibular second molars with a modified uprighter jet. J Clin Orthod. 2007;41:281-84.
41. Gu G, Lemery SA, King GJ. Effect of appliance reactivation after decay of initial activation on osteoclasts, tooth movement, and root resorption. Angle Orthod. 1999;69(6):515-22.
42. Andreasen GF, Zwanziger D. A clinical evaluation of the differential force concept as applied to the edgewise bracket. Am J Orthod Dentofac Orthop. 1980;78(1):25-40.
43. Romeo DA, Burstone CJ. Tip-back mechanics. Am J Orthod. 1977;72(4):414-21.
44. Smith RJ, Burstone CJ. Mechanics of tooth movement. Am J Orthod. 1984;85(4):294-307.
45. Nabbout F, Baron P. Anchorage in orthodontics: Three-dimensional scanner input. J Int Soc Prev Community Dent. 2018;8(1):6.
46. Proffit WR. The biologic basic of orthodontic therapy. In: Duncan L, ed: *Contemporary orthodontics.* 5th ed. Missouri: Elsevier/Mosby;2013:278-311.
47. Bondemark L, Tsiopa J. Prevalence of ectopic eruption, impaction, retention and agenesis of the permanent second molar. Angle Orthod. 2007;77(5):773-8.
48. Geng J-P, Tan KB, Liu G-R. Application of finite element analysis in implant dentistry: a review of the literature. J Prosthet Dent. 2001;85(6):585-98.
49. Piccioni MAR, Campos EA, Saad JRC, de Andrade MF, Galvão MR, Rached AA. Application of the finite element method in Dentistry. Rev Bras Odontol. 2013;10(4):369-77.

50. Mohammed S, Desai H. Basic concepts of finite element analysis and its applications in dentistry: An overview. Int J Dent Hyg. 2014:1-5.
51. Cattaneo P, Dalstra M, Melsen B. The finite element method: a tool to study orthodontic tooth movement. J Dent Res. 2005;84(5):428-33.